

# Fractal Assessment of Capacitating Spermatozoa in Video Sequences

**Pablo Odorico**

Departamento de Ciencias e Ingeniería de la Computación — Universidad Nacional del Sur — [pablo.odorico@gmail.com](mailto:pablo.odorico@gmail.com)

**Norbert Kaula**

Department of Computer Science — University of Denver — [nkaula@cs.du.edu](mailto:nkaula@cs.du.edu)

and

**Claudio Delrieux**

Instituto de Investigaciones en Ingeniería Eléctrica - IIIE (UNS-CONICET) —  
Departamento de Ing. Eléctrica y Computadoras — Universidad Nacional del Sur —  
[claudio@acm.org](mailto:claudio@acm.org)<sup>1</sup>

## Abstract

This work is aimed to develop tools for the robust, unsupervised assessment of fertility of sperm samples using video sequences, by means of an estimation of the proportion of hyperactivated spermatozoa in the sample. For this purpose, we developed a software tool for trajectory tracking in standard video takes of sperm samples. We discuss the steps of the tracking procedure and present some results. Then, we study two fractal characterizations for spermatozoa trajectories, the well known box counting dimension, and a new regression, which we call *time dependency fractal dimension*, which establishes a relationship between the length of the trajectory and the frame rate of the tracking.

**Keywords:** IMAGE AND VIDEO PROCESSING — VIDEO TRACKING — FRACTAL DIMENSION — SPERMATOZOA

## Resumen

En este trabajo se proponen metodologías y herramientas robustas para en análisis no supervisado de la fertilidad de muestras de semen a partir de secuencias de video. El método consiste en determinar la proporción de espermatozoides hiperactivados a partir de un análisis de sus trayectorias respectivas utilizando descriptores fractales. Para ello se desarrolló un algoritmo para el seguimiento automático de las trayectorias de los espermatozoides en la muestra. Se propone la aplicación de dos descriptores fractales para el análisis de estas trayectorias: la dimensión *box counting*, y un nuevo método de regresión, al que denominamos *dimensión fractal de la dependencia temporal*, que establece una relación entre la longitud de la trayectoria respecto de la resolución temporal de la secuencia de video.

**Palabras Clave:** PROCESAMIENTO DE IMÁGENES Y VIDEO — SEGUIMIENTO EN VIDEO — DIMENSIÓN FRACTAL — ESPERMATOZOIDES

---

<sup>1</sup>Partially funded by SECyT-UNS

# 1 INTRODUCTION

Determining the proportion of spermatozoa with hyperactivated motility under capacitating conditions is, among others, a very important assessment, since it has been correlated with successful in-vitro fertilization. For that reason, accurate estimations of the proportion of hyperactivated spermatozoa represent a crucial test.

Different indications of hyperactivated motility in video takes are being sought. Most research works in this direction rely on kinematic parameters that have been derived for the video systems currently used for movement analysis [9, 1, 10], in particular, an analysis of the path traced by the sperm head. The parameters used were originally derived from studying the movement of spermatozoa in seminal plasma [2], and include the curvilinear velocity (VCL), the amplitude of lateral head displacement (ALH), and many others.

However, there are several drawbacks in this approach. On one hand, a careful determination of quantitative values for these parameters is tedious, difficult, and must be done with human supervision. On the other hand, slight errors in measurement have been shown to lead to misclassification. For this reason, this approach cannot be considered a robust method.

Therefore, different motility indicators are being sought, that may lead to a more reliable, less assisted classification method. One of those indicators that has been less explored is to quantify the fractal dimension (FD) of the head trajectory. In [8] the definition of two different FD measurements are considered, which lead to a reasonably robust classification of hyperactivity in spermatozoa with trajectories whose FD was larger than 1.3. However, this method consistently produces false positives with circular trajectories, among other problems.

In this work we present some advances towards the full automatization of the capacitating assessment process. First, we developed an efficient tracking algorithm for an adequate digitalization of the spermatozoa trajectories in video sequences. This algorithm is fully automatic, and is based on a frame by frame segmentation on the local environment surrounding previously detected spermatozoa heads. Second, we investigate the usefulness of two other FD definitions, namely the *box counting dimension* [6, 3] and a regression of the rectified length of the trajectories with respect to frame rate, which we call the *time dependency fractal dimension*. We show the results of both the tracking algorithm and the FD of the trajectories, and compare our results with those available in the literature.

## 2 TRAJECTORY TRACKING IN VIDEO SEQUENCES

As stated above, the shape of the spermatozoa paths is critical for the assessment of their hyperactivated motility. The usual way of gathering this information is by manually tracking the trajectory of a single spermatozoon in a sample. This procedure is obviously tedious, slow, and error prone. Therefore, a much sought after procedure for providing

good amounts of reliable information is to extract spermatozoa's trajectories directly and automatically from video sequences.

For this reason, we developed an algorithm that is able to track several individual spermatozoa's trajectories in parallel. After the first frame is analyzed and the algorithm's parameters are initialized, the main work of the algorithm is to perform a frame-by-frame update procedure, where the parameters of the next frame are computed based on the information gathered from the previous frame. The parameters to be initialized and updated are essentially the actual positions of the spermatozoa's heads. The algorithm is able to track a user-determined amount of trajectories in parallel. Several aspects of this tracking procedure will be explained below.

## 2.1 Segmentation

We analyzed a set of video sequences and performed some supervised segmentations in order to find an adequate classifier in color space. It turned out to be that no simple color sample in the usual color spaces yielded a robust classifier. Euclid distance in color space from the most likely foreground color (spermatozoa's heads) was then used as a pixel descriptor. Therefore, the per-pixel segmentation procedure is to classify pixels as foreground only if the pixel descriptor (the distance in color space to the most likely foreground color) is below a threshold.

The tracking algorithm happened to be able to withstand false negatives better than false positives. For this reason, the threshold level (*i.e.*, the distance in color space of the pixel's color to an ideal sample) was set to an arbitrarily low value that makes false negatives far more frequent than false positives. The reason for this is self evident, since for an adequate tracking we only need to correctly classify some but not all of the pixels of the spermatozoa's heads, while having false positives may trigger inadequate initial conditions. Also, false positives make much more difficult the frame-by-frame update procedure.

## 2.2 Initialization procedure

The purpose of this step is to provide the initial positions of the spermatozoa's heads, enabling the frame-by-frame procedure to work only on an update basis. This procedure is applied to the first frame in the video sequence. This is the only frame in which the pixel descriptor introduced above is applied to every pixel in the frame.

Given a user-defined amount of  $n$  trajectories to track, this algorithm proceeds to find at most  $n$  clusters of pixels, all of which should satisfy two criteria:

1. All the pixels in a cluster are classified as foreground (*i.e.*, likely to belong to a spermatozoa's head), and
2. all the pixels in a cluster are 4-connected (have an edge in common).

This part of the procedure resembles the basin initialization step of the watershed algorithm [7].

The search for clusters is quite straightforward, and any systematic search procedure will fulfill the purpose. The amount of clusters satisfying the two criteria above might be different to the user-defined  $n$ . In case the former is larger than the latter, the procedure selects the most plausible  $n$ , according either to the amount of pixels in the cluster, or to how significantly the pixels in the cluster are below the classification threshold. This is because a connected set of positively classified pixels is less likely due to a false positive (the larger the set, the less likely a misclassification), and also because a connected set of pixels well close to the ideal foreground color is less likely due to a false positive (and the closer the color of the pixels to the ideal one, the less likely a misclassification). In case that the initialization is unable to find  $n$  or more clusters, the amount of trajectories to be tracked in the next steps is lowered to fit to the amount of clusters found to satisfy the two criteria above.

Finally, the most likely position of a spermatozoa's head is set to the centroid of each cluster, that is, the average  $x$  and  $y$  of the pixels belonging to the cluster.

### 2.3 Frame-by-frame Update

The key for the efficiency of the tracking algorithm is to be able to track the trajectories correctly, performing the least possible computations. As it will be explained later, the hyperactivation motility assessment does not require to track as many trajectories as possible, nor tracking them after a given amount of time has passed. Therefore, our algorithm's only concern is tracking the paths of the spermatozoa found in the initialization process described above, until they exit the sample viewport, or until the video sequence ends. In other words, in the update process there is no need to search for new trajectories or heads.

This, together with the fact that the FPS rate of the video is high enough (which must be for any result to be significant), implies that the update algorithm only needs to focus the search in the nearby of the centroids of the trajectories that are still active. In other words, the position of any spermatozoa's head in the next frame is certainly going to be very close to the centroid of the cluster already found in the previous frame. This principle is violated only in two circumstances:

1. The path exits the frame's boundaries. This case can easily be checked if the cluster centroid is close to the boundaries in the previous frame, and the amount of positively classified pixels in the cluster close to that centroid diminishes or completely vanishes.
2. Two or more paths intersect. This case requires additional considerations that will be explained in the next Subsection.

Therefore, the complete update procedure can be summarized as follows:

1. For each trajectory that was active in the previous frame, given the centroid  $x, y$  of the cluster, compute a description for the pixels in the next frame that are at distance  $d$  to that centroid.
2. Classify the connected set of pixels below the average distance to the ideal foreground as the new cluster associated to the trajectory in the next frame.
3. If no satisfactory cluster is found, and the centroid in the previous frame was close to the frame's boundaries, then assume that the path exits the viewport and terminate the tracking for this trajectory.

This frame-by-frame procedure goes on until all the trajectories are terminated, or the frame sequence ends. The output is the sequence of the centroids that were computed for each trajectory.

## 2.4 Intersection management

Eventually, the paths of two or more spermatozoa's heads may intersect. This may cause that the clusters of positively classified pixels associated to the spermatozoa's heads merge together. Therefore, additional considerations should be taken to be able to discern the evolution of the trajectories after the intersection.

A naïve idea would be to mark such a cluster as pertaining to all the trajectories participating in the intersection, and after the paths split, then associate back the clusters to the trajectories. However, there is a certain risk of crossover in the tracking, since there is no way of discerning to which trajectory a cluster pertains after the intersection. Such a crossover would undermine all the motility assessment procedure, and therefore should be avoided.

To cope with this problem, a regression was performed considering a few of the previous centroids' positions in the intersecting trajectories. In all the cases considered in our research, a linear regression was enough to adequately disambiguate the adscription of clusters to trajectories after the intersection (see [http://www.youtube.com/watch?v=C\\_icae0Qr0k](http://www.youtube.com/watch?v=C_icae0Qr0k) for an example). However, if needed, a higher order regression can be computed.

This approach may fall completely if two or more spermatozoa's paths move together for some consecutive frames, even though in our research we never found a situation like this to occur. If the disambiguation is not successful, then the tracking of all the intervening trajectories is terminated.

## 2.5 Some Results

All the steps in our tracking algorithm are implemented in **STrack**, a software tool for tracking spermatozoa trajectories in video sequences. In Fig. 1 we show a screenshot of this tool where the initialization procedure was applied to the first frame in a sequence,

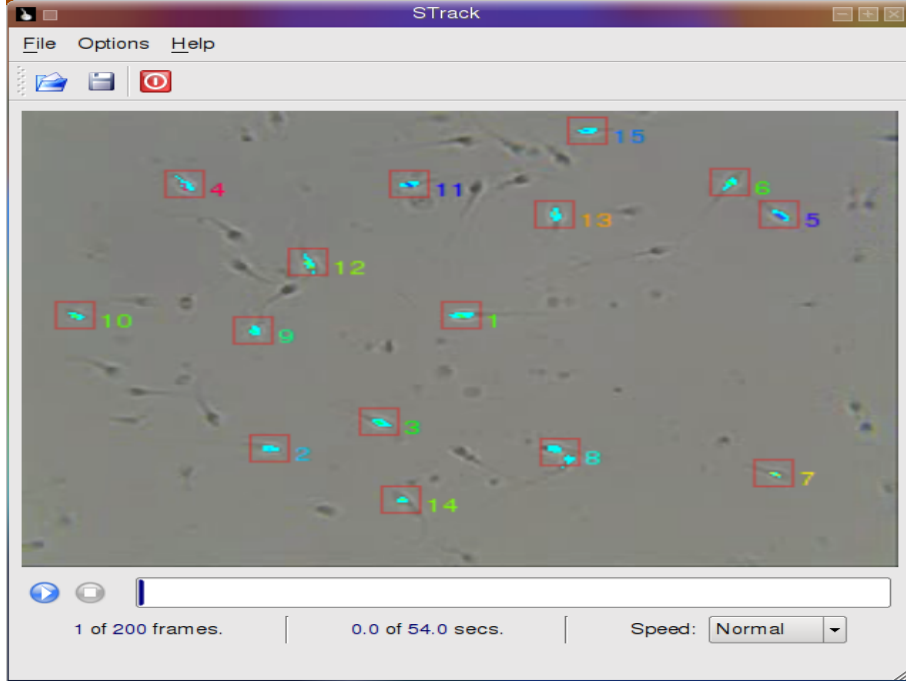


Figure 1: First frame in a video sequence after the initialization procedure.

and  $n$  was set to 15. We used false color to paint the 15 basins detected at this initialization procedure as the most plausible locations for spermatozoa's heads.

In Fig. 2 the tracking result after the update of 80 frames is shown. The trajectories are also shown with false color. The complete video sequence can be found at <http://www.youtube.com/watch?v=o53t0tD2MFU>.

### 3 FRACTAL ANALYSIS OF TRAJECTORIES

The fractal characterization of geometric object has been intensively studied since Mandelbrot's introduction of these ideas in the 1970s [5, 4]. In images, as well as in other non-deterministic sets, there is a close relationship between the fractal properties and the inherent geometrical properties of the set [11]. This relationship suggests the possibility of computing an indirect estimation of the fractal dimension using statistical methods that extend the usual definitions of fractality. In our case, we are exploring fractal descriptors of spermatozoa's trajectories.

The basis for fractal dimension analysis is the concept of Hausdorff self-similarity measure, or Hausdorff fractal dimension. A closed set  $A$  in an affine space is *self-similar* if  $A$  can be expressed as the union of  $N(r)$  not overlapping copies of itself scaled with a scaling ratio  $r$ . In this case, the Hausdorff (or self-similarity) dimension  $D_h$  of  $A$  is given by the relationship:

$$D_h = \lim_{r \rightarrow 0} \frac{\log(N(r))}{\log(\frac{1}{r})}. \quad (1)$$

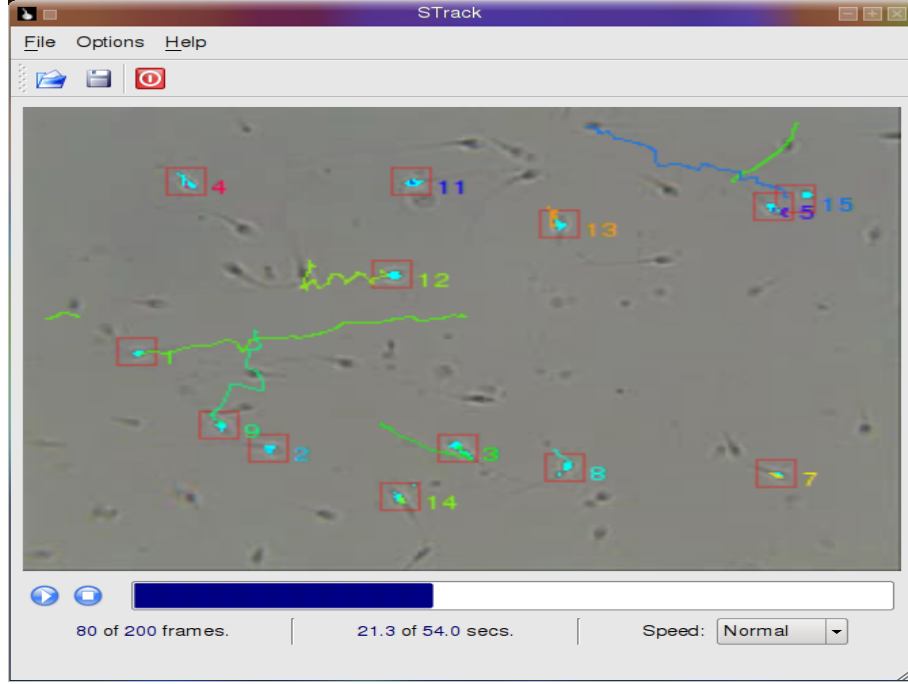


Figure 2: Tracking after 80 frames.

Eq. 1 is the basis of the estimation of the fractal dimension of arbitrary sets in an abstract space. However, because its generality it is of little computational use. Several alternative methods are proposed in the literature to compute the fractal dimension of sets. In image processing, most of them are applied to previously binarized images, since a binarized image can be regarded as the set of lit pixels in an affine subspace of  $\mathbb{R}^2$ , and, in our case similar considerations can be applied to a path or trajectory [13].

A particularly useful fractal dimension used for characterizing linear features is the *compass* dimension, which was successfully used in the analysis of geographical features as rivers, coastlines, borderlines, and so on. The compass dimension is the regression in a log-log space of the length  $long(l)$  of the rectification of the feature computed with a polyline of side  $l$ , when the length of  $l$  goes to zero:

$$D_c = \lim_{l \rightarrow 0} \frac{\log(long(l))}{\log(1/l)}. \quad (2)$$

In other words,  $D_c$  is the exponent that relates the measured length of the feature with respect to the width of a compass or dividers used to establish that length. The compass dimension is more amenable to computer implementation. Also, the relationship with the Hausdorff dimension  $D_c = D_h - 1$  is easy to verify<sup>2</sup>.

Several other fractal characterizations are available in the literature. In particular, for fractal assessment of spermatozoa trajectories, Mortimer et. al. [8] propose an alternate definition that considers also the amount  $n$  of samples in the tracking of the trajectory,

---

<sup>2</sup>If we take the scaling factor  $r$  in  $D_h$  to be equal to the dividers length  $l$  in  $D_c$ . In this case it follows that  $long(l) = N(r)l$ . Now, it follows  $D_c = \lim_{l \rightarrow 0} \frac{\log(long(l))}{\log(1/l)} = \lim_{l \rightarrow 0} \frac{\log(N(l)l)}{\log(1/l)} = \lim_{l \rightarrow 0} \frac{\log(N(l)) - \log(1/l)}{\log(1/l)} = \lim_{l \rightarrow 0} \frac{\log(N(l))}{\log(1/l)} - 1 = D_h - 1$ .

and the planar extension  $d$  of the rectangle that properly contains it:

$$D_m = \frac{\log(n)}{\log(n) + \log(d/l)}. \quad (3)$$

This authors compute  $D_m$  for a given trajectory, with  $n$ ,  $l$ , and  $d$  fixed (i.e., no regression is considered, which is methodologically questionable), and arrive into the conclusion that hyperactivated trajectories are such that  $D_m \geq 1.3$ , while non-hyperactivated trajectories have a  $D_m$  value below 1.2 (with the exception of circle-like trajectories). These preliminary results confirm the idea that a fractal characterization of trajectories may be a good motility indicator.

In this work we studied another two fractal characterization of sets. The first one is the well known occupancy dimension, or *box* fractal dimension (BFD). In BFD,  $N(r)$  is the amount of cells of radius  $r$  that are occupied by the set. Given a binarized image of  $M \times M$  pixels, we subdivide the image in grids of  $s \times s$ , where  $M/2 \geq s > 1$  and  $s \in \mathbb{Z}$ . Then, the space  $(x, y)$  is partitioned with cells of size  $s$ . In this case the radius is  $r = s/M$ . If some lit pixel of  $A$  is within a cell, we consider that the cell is occupied, and  $N(r)$  is incremented. The final value of  $N(r)$ , then, is obtained counting up all the cells of the grid that contained at least one lit pixel.  $N(r)$  it is computed for different radii  $r$ , averaging the counts over grids superimposed in different positions of the image. Then, the BFD, ideally defined as

$$D_b = \lim_{r \rightarrow 0} \frac{\log(N(r))}{\log(1/r)}, \quad (4)$$

can be estimated as the slope of the least squares regression that fits the scatter plot of  $\log(N(r))$  vs.  $\log(1/r)$  [12].

The second characterization regards the dependency of the level of detail in the trajectory with respect to the FPS rate in the video sequence. For this reason, we call it the *time dependency fractal dimension*  $D_t$ . The underlying idea in establishing  $D_t$  is that the level of detail of a trajectory will be sampled to greater detail with a higher FPS rate. However, this dependency is not going to be even for all trajectories. On the contrary, the growth in detail with respect to frame ratio is going to be higher in fuzzier, more rough paths, and lower in smoother ones.

Assuming that the length of the rectification of a trajectory is a rough estimate of its level of detail, we compute the length  $\text{long}(t)$  of the trajectory with respect to a FPS rate  $t$ . If the available video sequence has a FPS  $f$  (usually 60 Hz.), it means that the time interval in seconds between frames is  $\delta t = 1/f$ . Then, we can establish the length of the rectified trajectory under different undersampling rates, simply taking  $t = k\delta t$ . For instance, if the original video sequence is of 60 Hz., then taking  $k = 2$  will provide a trajectory sampling at 30 Hz., taking  $k = 3$  will provide a trajectory sampling at 20 Hz., and so on.

With those considerations in mind, we can finally establish our time dependency fractal dimension as

$$D_t = \lim_{t \rightarrow 0} \frac{\log(\text{long}(t))}{\log(1/t)}. \quad (5)$$

In other words,  $D_t$  is an exponent that relates the growth in level of detail with respect to the increase of the sampling rate in the video sequence. Again, a regression that fits a scatter plot of these values provides a good approximation of  $D_t$ .

## 4 RESULTS

Both the tracking algorithm and the fractal estimators exhibited a robust behavior. In Fig. 3 we show some of the trajectories (rotated to fit in the page, and with time encoded as a pseudo color) that were computed using the algorithm in the previous Section.

In Fig. 4 we show part of the procedure of computing the BFD of a trajectory. In that Figure, different levels of subdivision are shown, and for each, the cells occupied by the trajectory are highlighted. In Fig. 5 we show the initial four undersampling rates in computing the time dependency fractal dimension, and the resulting rectified trajectories.

In Table 1 we show the result of applying these two fractal dimensions to the trajectories shown in Fig. 3. These results show that the fractal estimators are able to characterize adequately the geometric features of the trajectories.

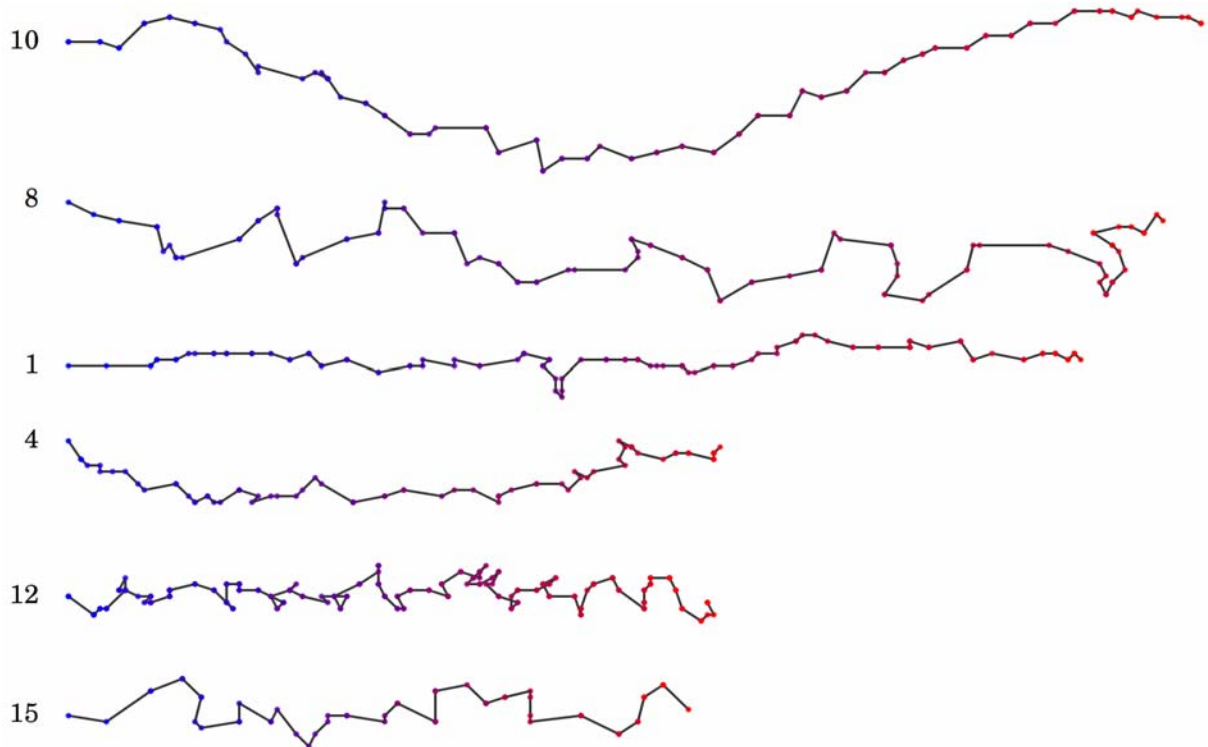


Figure 3: A set of trajectories obtained with the tracking algorithm, identified by number.

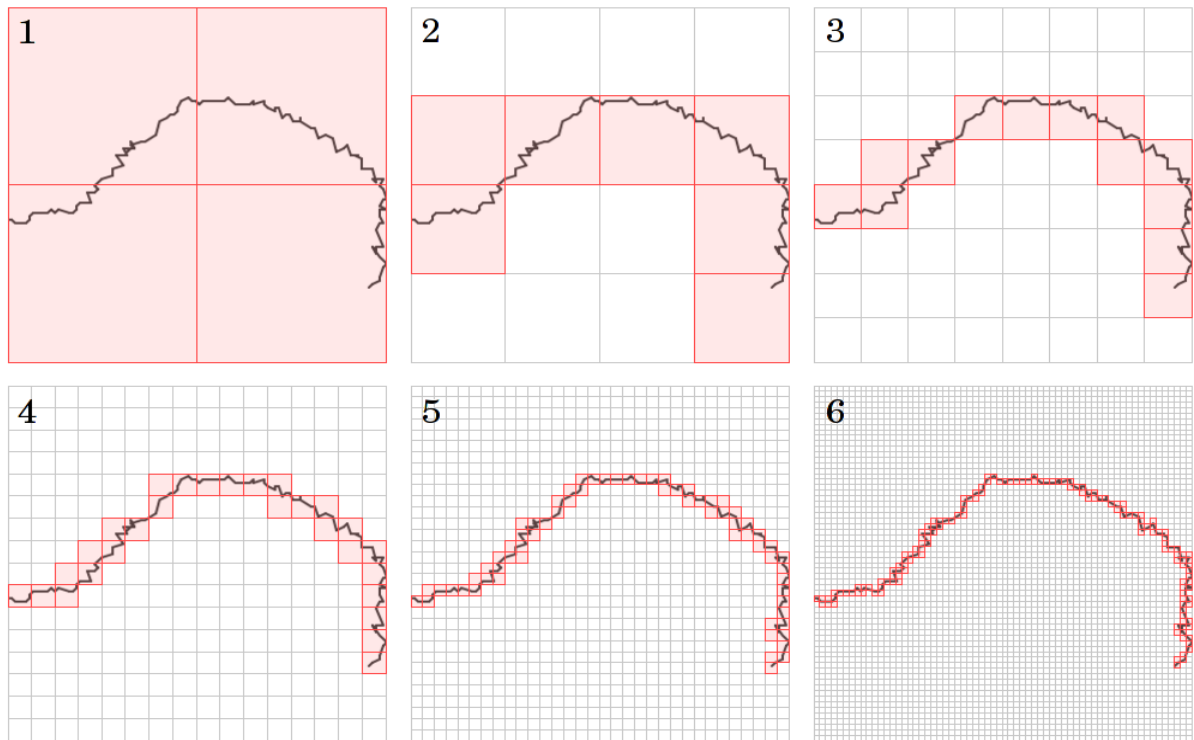


Figure 4: Several subdivision levels in computing the BFD, and the occupied cells at each level.

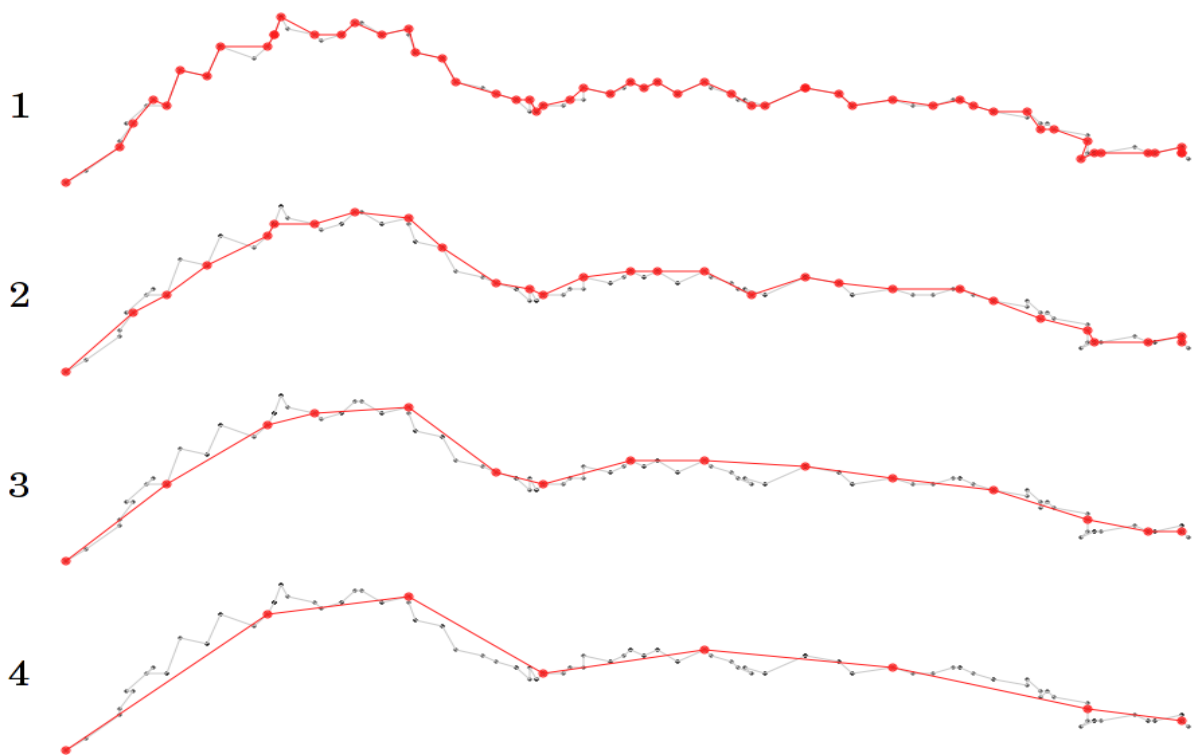


Figure 5: A trajectory under four undersampling rates, and the resulting rectifications.

Trayectory	$D_t$	$D_b$
10	1.13911	1.01489
8	1.20840	1.07117
1	1.14355	1.05294
4	1.17517	1.03801
12	1.27538	1.18789
15	1.35917	1.11135

Table 1:  $D_t$  and  $D_b$  fractal dimensions for the trajectories in Fig. 5.

## 5 CONCLUSIONS AND FUTURE WORK

We presented the results of a system aimed at the unsupervised assessment of the fertility of sperm samples using video sequences. We developed a software tool for trajectory tracking in standard video takes of sperm samples. Two fractal characterizations for spermatozoa trajectories were applied, the well known box counting dimension, and a new regression, which we called *time dependency fractal dimension*, which establishes a relationship between the length of the trajectory and the frame rate of the tracking.

The next steps in our research are to enhance the tracking algorithm to be able to analyse as many spermatozoa's paths as possible, and to compute a statistical distribution of the fractal dimensions of their trajectories. This, in turn, will allow a classification of the proportion of hyperactivated trajectories in the sample, and therefore decide the potential fertility of the sample.

## References

- [1] L.J. Burkman. Discrimination between nonhyperactivated and classical hyperactivated motility patterns in human spermatozoa using computerised analysis. *Fertil. Steril.*, 55:363–371, 1991.
- [2] R.O. Davis and R.J. Siemers. Derivation and reliability of kinematic measures of sperm motion. *Reprod. Fertil. Dev.*, 7:857–869, 1995.
- [3] H. Jürgens H.-O. Peitgen and D. Saupe. *Chaos and Fractals: New Frontiers of Science*. Springer-Verlag, New York, 1992.
- [4] M.J. Katz. Fractals and the analysis of waveforms. *Comput. Biol. Med.*, 18:145–156, 1988.
- [5] B. Mandelbrot. *Fractals: Form, Chance and Dimension*. W. H. Freeman, New York, 1977.
- [6] B. Mandelbrot. *The Fractal Geometry of Nature*. W. H. Freeman, New York, 1983.
- [7] Fernand Meyer. Topographic distance and watershed lines. *Signal Processing*, 38:113–125, July 1994.

- [8] M.A. Mortimer, S.T. Swan and D. Mortimer. Fractal analysis of capacitating human spermatozoa. *Human Reproduction*, 11(5):1049–1054, 1996.
- [9] S.T. Mortimer and D. Mortimer. Kinematics of human spermatozoa incubated under capacitating conditions. *J. Androl*, 11:195–203, 1990.
- [10] S.T. Mortimer and M.A. Swan. Kinematics of capacitating human spermatozoa analysed at 60 Hz. *um. Reprod.*, 10:873–879, 1995.
- [11] H.-O. Peitgen and D. Saupe. *The Science of Fractal Images*. Springer-Verlag, New York, 1988.
- [12] J. C. Russ. *The Image Processing Handbook*. CRC Press, Boca Raton, FL, third edition, 1999.
- [13] Pierre Soille and Jean-F. Rivest. On the validity of fractal dimension measurements in image analysis. *J. Visual Communication and Image Representation*, 7(3):217–229, 1996.